



**UvA-DARE (Digital Academic Repository)**

**Pulse delay observations of GRO J1744-28**

Koshut, T.M.; Kouveliotou, C.; van Paradijs, J.A.; Woods, P.; Fishman, G.J.; Briggs, M.S.; Lewin, W.H.G.; Kommers, J.M.

*Published in:*  
Astrophysical Journal

*DOI:*  
[10.1086/311254](https://doi.org/10.1086/311254)

[Link to publication](#)

*Citation for published version (APA):*

Koshut, T. M., Kouveliotou, C., van Paradijs, J. A., Woods, P., Fishman, G. J., Briggs, M. S., ... Kommers, J. M. (1998). Pulse delay observations of GRO J1744-28. *Astrophysical Journal*, 496, L101-L104. DOI: 10.1086/311254

**General rights**

It is not permitted to download or to forward/distribute the text or part of it without the consent of the author(s) and/or copyright holder(s), other than for strictly personal, individual use, unless the work is under an open content license (like Creative Commons).

**Disclaimer/Complaints regulations**

If you believe that digital publication of certain material infringes any of your rights or (privacy) interests, please let the Library know, stating your reasons. In case of a legitimate complaint, the Library will make the material inaccessible and/or remove it from the website. Please Ask the Library: <http://uba.uva.nl/en/contact>, or a letter to: Library of the University of Amsterdam, Secretariat, Singel 425, 1012 WP Amsterdam, The Netherlands. You will be contacted as soon as possible.

## PULSE DELAY OBSERVATIONS OF GRO J1744–28

T. M. KOSHUT,<sup>1,2</sup> C. KOUVELIOTOU,<sup>1,2</sup> J. VAN PARADIJS,<sup>3,4</sup> P. M. WOODS,<sup>2,3</sup> G. J. FISHMAN,<sup>2</sup> M. S. BRIGGS,<sup>2,3</sup>  
W. H. G. LEWIN,<sup>5</sup> AND J. M. KOMMERS<sup>5</sup>

Received 1997 October 31; accepted 1998 January 27; published 1998 February 24

### ABSTRACT

The bursting pulsar GRO J1744–28 exhibits a unique combination of persistent X-ray pulsations (with a pulse period  $P_{\text{pulse}} \approx 0.467$  s) and X-ray bursts. The pulsations are also present (at an enhanced amplitude) during the bursts, but the arrival times of the pulses during the burst are delayed with respect to those of the persistent emission. We present the results of a detailed study of the pulse delays using data obtained with the Burst and Transient Source Experiment on board the *Compton Gamma Ray Observatory*. We find that the average delay, as measured during a 1.5 s interval at the peak of the burst, is independent of energy in the energy range  $\sim 25$ –75 keV and has a magnitude  $\langle \Delta t \rangle = 74 \pm 13$  ms. We also find that the phase delay measured near the peak of the bursts remained approximately constant throughout the first outburst of the source, although the peak flux of the bursts varied by a factor of  $\sim 3.3$ .

*Subject headings:* binaries: general — gamma rays: observations — pulsars: individual (GRO J1744–28) — X-rays: bursts

### 1. INTRODUCTION

The bursting pulsar was discovered with the Burst and Transient Source Experiment (BATSE) on board the *Compton Gamma Ray Observatory* (CGRO) on 1995 December 2 (Fishman et al. 1995; Kouveliotou et al. 1996b). On that day, X-ray bursts were observed at a rate of  $\sim 20$  hr<sup>-1</sup>; thereafter, they were detected at a rate of  $\sim 20$  day<sup>-1</sup> until about 1996 April 27. A persistent X-ray source whose position was consistent with the source of the X-ray bursts was found on 1995 December 12 (Paciesas et al. 1996). X-ray pulsations, with a period  $P_{\text{pulse}} \approx 0.467$  s, were first observed in the persistent emission on 1995 December 15 (Finger et al. 1996). Later analysis shows that the pulsations were already present in the archival data on 1995 December 1 (Finger 1996). The pulse profile is nearly sinusoidal in the energy band 20–40 keV, with a first harmonic observed at an amplitude of  $6.2\% \pm 0.6\%$ . The observation of the 0.467 s pulsations with strongly enhanced amplitude during the bursts has associated the persistent and burst emission with the same source (Kouveliotou et al. 1996a). The orbital period  $P_{\text{orb}} = 11.8$  days (Finger et al. 1996) and the low value of its mass function [ $f_{\text{X}}(M) = 1.37 \times 10^{-4} M_{\odot}$ ] indicate that the system is a low-mass X-ray binary. A second outburst of both persistent and burst emission, similar in character to the first outburst, was observed to begin on 1996 December 2, lasting until the end of April.

Using data obtained with the Oriented Scintillation Spectrometer Experiment (OSSE) on board CGRO, Jung et al. (1996) and Strickman et al. (1996) found that during the bursts, the pulsations lag those in the persistent emission, with a maximum time lag of  $\Delta t \approx 90$  ms occurring at the time of the burst peak, settling to a lag of  $29 \pm 6$  ms during the interval 10–80 s after the burst onset in the OSSE data. Independently, Stark

et al. (1996) used data obtained with the Proportional Counter Array (PCA) on board the *Rossi X-Ray Timing Explorer* (RXTE) to measure phase delays during the burst; these phase delays were consistent with those observed in the OSSE data. However, observations during the burst were complicated by uncertain corrections for instrument dead time. They show that following the bursts, when dead-time corrections were insignificant, the phase shift decays exponentially, with a typical decay time of several hundred seconds. Although observations were often interrupted by Earth occultation, they did observe a complete phase recovery (to the preburst value) in some bursts.

In this Letter, we report on BATSE observations of the phase shifts during the burst emission. We examine the energy dependence of the average phase shift  $\Delta t$ . We present the variation of the phase shifts  $\Delta t$  during the average burst, as well as the evolution of the average phase shift  $\langle \Delta t \rangle$  throughout the first outburst. Analysis of the phase delays during the second outburst will be presented in a future paper (Woods et al. 1998).

### 2. BATSE OBSERVATIONS OF GRO J1744–28

The data used here were obtained with the BATSE Large Area Detectors and span the energy range of  $\sim 20$ –2000 keV. These data consist of 16 energy channels, with a time resolution of 2.048 s prior to the event trigger time  $t_{\text{trg}}$ , 16 ms from  $t_{\text{trg}}$  to  $t_{\text{trg}} + 32.768$  s, 64 ms from  $t_{\text{trg}} + 32.768$  s to  $t_{\text{trg}} + 163.84$  s, and 2.048 s afterward. Further details on BATSE and the various data types can be found in Fishman et al. (1989).

In this study, the 2.048 s time resolution data are used only for background modeling. The 16 ms data are used to measure the phase shifts during the bursts but are available only for those events that satisfied the on-board triggering criteria. The nominal triggering energy range (50–300 keV) was extended down to  $\sim 25$  keV on 1995 December 11 in order to optimize the triggering criteria for the bursting pulsar events.

BATSE triggered on 1350 bursts from GRO J1744–28 between 1995 December 2 and 1996 April 3. Of this sample, 16 ms data were available for 649 events (depending on the BATSE data readout schedule in use). Before 1996 January 10, 16 ms data were available only for events that were at least  $10 \sigma$  above background at  $t_{\text{trg}}$ . Between 1996 January 10 and

<sup>1</sup> Universities Space Research Association.

<sup>2</sup> NASA/Marshall Space Flight Center, ES-84, Huntsville, AL 35812; Thomas.Koshut@msfc.nasa.gov.

<sup>3</sup> Department of Physics, University of Alabama at Huntsville, Huntsville, AL 35899.

<sup>4</sup> Astronomical Institute “Anton Pannekoek,” University of Amsterdam, Kruislaan 403, 1098 SJ Amsterdam.

<sup>5</sup> Department of Physics, Center for Space Research, MIT, Cambridge, MA 02139.

30, these data were output only for events that were at least  $20\sigma$  above background. Afterward, the 16 ms data were output for all triggered events. Incomplete data due to telemetry gaps and interference from other sources prevented the use of some triggered events, limiting the number of events with 16 ms data that were analyzed to 406.

### 3. DATA ANALYSIS PROCEDURE

Phase shifts could not be examined with sufficient precision for a single burst; therefore, it was necessary to sum bursts together. The profile shapes of the bursts observed after the first 2 days varied substantially from those observed during the first 2 days of observations. Afterward, profile shape variation was observed, but the average burst profile remained constant, with variation only in peak intensity.

Prior to summing, each burst was subjected to a procedure that removed the long-term background flux, subtracted the underlying burst envelope (leaving only the residual pulsed flux), and phase-aligned the residual pulsed flux with other bursts.

First, an interval of background data, usually at least  $\sim 100$  s in duration, was defined both prior to and following each burst. These data were fitted to a second-degree polynomial model, although a higher order polynomial was used in four of the 406 bursts. This model was interpolated between the two background intervals and subtracted from the data.

The effects of variations in burst profile shapes were minimized by passing the background-subtracted bursts through a digital high-pass filter (Walraven 1984) of order 100, with a low-frequency cutoff of 1.516 Hz. This filter required that the data have a constant time resolution. Therefore, prior to the application of the filter, the time resolution of the coarser resolution data was converted to 16 ms. The count rates of the rebinned data were assumed to be equal to the count rate observed in the coarser data. Woods et al. (1998) will present a detailed study of the systematics associated with the filtering process.

After the de-trending, each burst was phase-aligned. We used the persistent flux ephemeris (M. H. Finger 1996, private communication) to identify the first expected occurrence time, after  $t_{\text{trg}}$ , of phase  $\phi = 0$  ( $\phi$  is defined in the persistent ephemeris such that the pulse maximum corresponds to  $\phi = 0.25$ ). Data prior to this time are truncated from the time history.

These phase-aligned burst time histories can be combined to study the behavior of the phase shift during the burst emission. This is done by averaging the observed count histories from multiple phase-aligned bursts. The time period over which the bursts are combined is dependent upon the scientific goal of the study, and this will be addressed later. For the moment, we assume that we have a background-subtracted, de-trended, phase-aligned burst time history resulting from an average over multiple bursts. Figure 1a shows such a profile, summed over the energy range of  $\sim 25$ –75 keV, for 291 bursts that were observed over the time period of 1995 December 24–1996 March 6. A train of pulses with a period approximately equal to  $P_{\text{pulse}}$  can clearly be identified. It is also obvious that the pulse amplitude is enhanced during the burst. This enhancement can be seen in many individual burst time histories as well.

To calculate the phase shift, a pulse profile template, one cycle of a sinusoid with a period  $P_{\text{pulse}}$ , is created with 16 ms time resolution. The first point of the template is aligned with the first data point in the averaged burst profile. The value of the Pearson correlation coefficient  $r$  is calculated using the

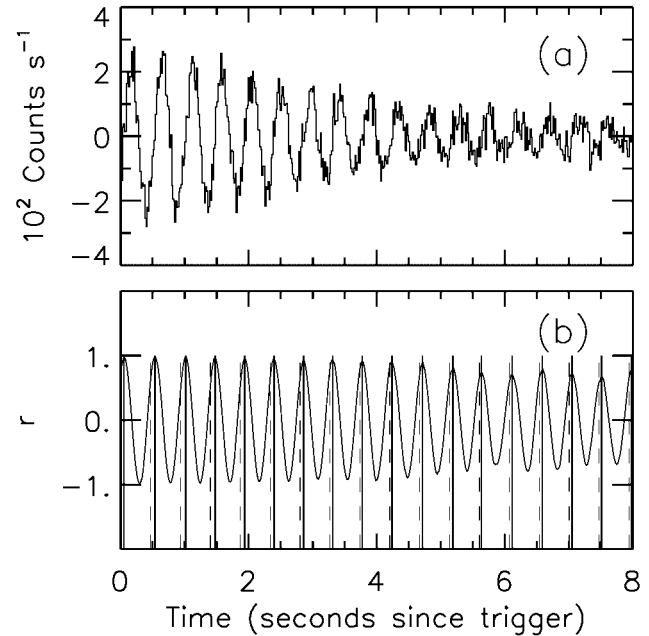


FIG. 1.—(a) The background-subtracted, de-trended, time history resulting from averaging 291 bursts, observed between 1995 December 24 and 1996 March 6, and summing over the energy range of  $\sim 25$ –75 keV; (b) Pearson correlation coefficient  $r(t)$  as a function of time using the time history shown in (a). The dashed (solid) vertical lines indicate the expected (observed) times of the peaks in  $r(t)$ .

template profile and the first cycle of data points. The template is slid forward one data point, and  $r$  is again calculated. The template is slid through the remaining fine time resolution data of the averaged burst profile, calculating  $r$  at each point, thus providing the correlation coefficient  $r(t)$ . If the data were identically sinusoidal, then the values of  $r(t)$  would vary between 1 and  $-1$  as the template varied between being in phase and being half a cycle out of phase, respectively, with the data.

Figure 1b shows a plot of  $r(t)$  calculated using the data shown in Figure 1a. The peaks (valleys) in  $r(t)$  are an indication of the best (worst) alignment between the template pulse profile and each cycle in the average burst profile. The expected periodic variations in  $r(t)$  are evident; the magnitude of  $r(t)$  never reaches unity because of the existence of Poisson fluctuations in the averaged burst profile.

To estimate the times of the observed peaks and valleys in the time profile of  $r(t)$ , we first searched for changes in the sign of the slope of  $r(t)$ . We required that the points immediately prior to and following any valid change in the sign of the slope were consistent with the sense of the sign change. We did not impose any a priori requirements about the order of observed sign changes; our algorithm to find changes in slope did not require a valley between two observed peaks. We then fitted  $\sim 300$  ms of data surrounding each sign change to a parabolic model. The centroid of the resulting best fit was then taken as the observed time of the peak or valley (these times are indicated by the solid vertical lines in Fig. 1b; for clarity, the lines associated with the valleys have been omitted). The time delays  $\Delta t$  were then calculated as the difference between the time (shown in Fig. 1b as the dashed vertical lines) of the peak (valley) predicted from the persistent flux ephemeris and the observed time of the peak (valley), measured as just previously described.

To verify that the phase shifts calculated were not syste-

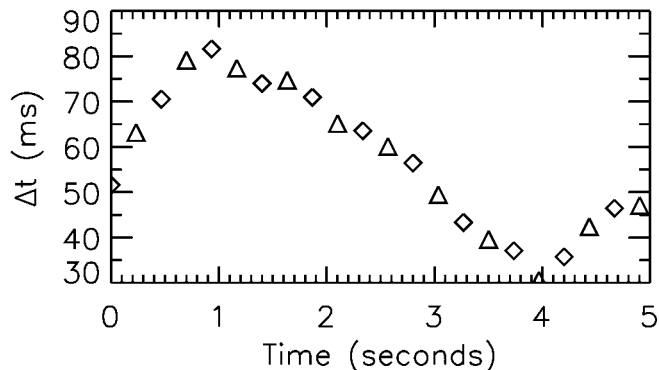


FIG. 2.—The evolution of the phase delay  $\Delta t$  through the average burst profile for the same bursts used to make Fig. 1a, summed over the energy range of 25–60 keV. The diamonds and triangles represent the phase delays determined using the observed peaks and valleys, respectively.

matically affected by our method, we simulated pulsed signals with three different models: (1) purely periodic, with no phase shift, (2) a constant phase shift of  $\Delta t = 20$  ms, and (3) a phase shift that varies over time, starting at  $\Delta t = 90$  ms and linearly decaying over 7 s to a stable value of  $\Delta t = 20$  ms. We applied the previously described method to each model and found very good agreement between the measured results and the input model. In each of the three cases, the uncertainty on the first measured phase shift was larger than that in subsequent measurements by a factor of  $\sim 2$  because of the fewer number of data points in the parabolic fit when trying to determine the location of the first peak of  $r(t)$ .

#### 4. RESULTS AND DISCUSSION

We averaged 16 ms data for 291 bursts in phase, observed over the time period of 1995 December 24–1996 March 6, as described in the previous section. We then summed the data over the energy range of  $\sim 25$ –60 keV. Because the phase delay is independent of energy (see below), summing over energy allowed us to increase our signal-to-noise ratio. We were able to further increase the signal-to-noise ratio by limiting the upper threshold of the energy range to 60 keV. In Figure 2, we show the temporal evolution of the phase delay  $\Delta t$  through the resulting average burst profile. The diamonds and triangles represent measurements made using the peaks and valleys, respectively, of  $r(t)$ . It can be seen that the phase delay  $\Delta t$  increases during the rise of the average burst profile, reaches a maximum of  $\sim 80$  ms near the peak of the profile, and then decreases with the decay of the burst profile (behavior qualitatively similar to that reported in Strickman et al. 1996 and Stark et al. 1996). The average phase delay  $\langle \Delta t \rangle$ , summed over a 1.5 s interval near the peak of this average burst profile, is  $\langle \Delta t \rangle = 77 \pm 8$  ms. (Using simulations, we found that the filtering process systematically lowered the first measured phase shift, and therefore the 1.5 s interval used for the averaging began at 0.5 s into the average profile.) The signal-to-noise ratio of the pulsed flux was too low for the 16 ms data to be of any use for measurements of the phase delay following the burst (time  $t \geq 4$  s in Fig. 2).

To investigate the energy dependence of the phase delays  $\Delta t$  in our energy range, we averaged the 16 ms data for the same 291 bursts in phase, without summing over energy. We averaged  $\Delta t$  over the same 1.5 s near the peak of the average burst profile in each energy channel. Figure 3 shows the re-

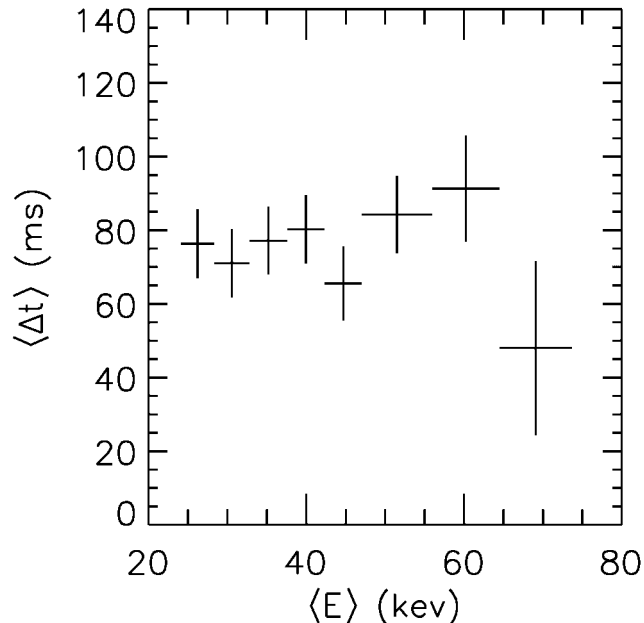


FIG. 3.—The energy dependence of the phase delay  $\Delta t$  using the same 291 bursts of Figs. 1 and 2.

sulting plot of  $\langle \Delta t \rangle$  as a function of energy. The data are consistent with the phase shift being independent of energy in the energy range of  $\sim 25$ –75 keV. Using the data, we find that  $\langle \Delta t \rangle = 74 \pm 13$  ms. In this Letter, the quoted errors on average phase delays include systematic contributions, taking into account the uncertainty in each individual phase delay measurement, and statistical contributions, using the observed sample variance to account for the finite sampling of parent distributions.

We have also examined the temporal dependence of  $\langle \Delta t \rangle$ , summed over energy, throughout the first outburst (1995 December 24–1996 March 31). The solid points in Figure 4 show  $\langle \Delta t \rangle$  as a function of time. As before, the averages were calculated over the same 1.5 s interval near the peak of the average burst profile, summed over the energy range of  $\sim 25$ –60 keV, during each time period. The results in Figure 4 show that the phase delay near the peak of the average burst remained approximately constant, in spite of the factor of  $\sim 3.3$  decrease in burst peak flux between 1996 January 13 and April 3. This result has been confirmed (Woods et al. 1998) using a data type with 64 ms time resolution, a slightly different procedure to calculate the phase shifts, and a larger sample of bursts.

There is perhaps a slight systematic decrease through the outburst in the measured  $\langle \Delta t \rangle$  for the 16 ms data. However, this can be attributed to the decreasing intensity (Briggs 1996) of the bursts after 1996 February. As the bursts became weaker, BATSE triggered later into the bursts. It has already been shown that the magnitude of the phase delay during bursts rises within a few seconds to a maximum and decreases thereafter (see Fig. 2). Thus, later in the outburst when the bursts are weaker and the trigger time occurs later in the burst, the peak of the average burst profile consists of pulses from portions of the burst where the phase delay is already decreasing. Averaging  $\Delta t$  near the peak of this average profile will result in a systematically smaller measurement of  $\langle \Delta t \rangle$ .

If the previous explanation is valid, we should be able to introduce this triggering effect into the earlier data (TJD

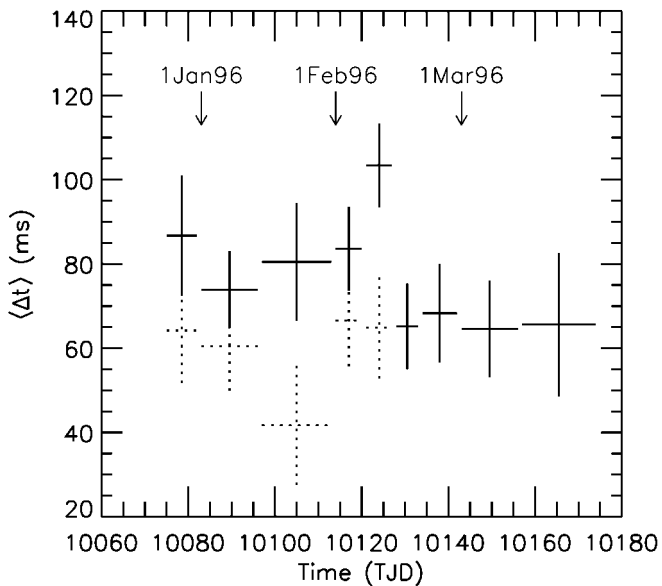


FIG. 4.—The solid data points show the average phase delay  $\langle \Delta t \rangle$  as a function of time through the first outburst of GRO J1744–28. The dashed points result from calculating the average phase delay  $\langle \Delta t \rangle$  later in the burst, thus simulating an artifact of the BATSE trigger (as the bursts become weaker, BATSE triggers later into the burst; see text).

10,070–10,127) by pretending that BATSE triggered later than it actually did. Early in the outburst when the bursts were most intense, BATSE typically triggered  $\approx 2$  s before the peak of the burst (we will call this time the *nominal* trigger time). If one assumes that the rise times of the bursts are nearly constant throughout the entire outburst, then the latest time into a weaker burst at which BATSE would be likely to trigger is at the time of the event peak count rate, which is approximately 2 s past the *nominal* trigger time. We introduced this effect into the earlier data by calculating  $\langle \Delta t \rangle$  over the 1.5 s interval beginning 2 s after the start of the 16 ms data of the average burst profile rather than the 1.5 s interval beginning at 0.5 s, as was done to produce the solid points in Figure 4. The start time of this interval, although somewhat ad hoc, was taken as the latest likely BATSE trigger time in order to produce qualitatively the effect of triggering later into the burst. The data are shown as the dotted points in Figure 4; the values of  $\langle \Delta t \rangle$  over this time period decreased to  $\approx 60$  ms, which is comparable to the level observed after TJD 10,127. We therefore conclude that the average phase shift remains constant throughout the outburst.

As argued by Kouveliotou et al. (1996b) and Lewin et al. (1996), the bursts from GRO J1744–28 are due to an accretion instability; i.e., they are type II bursts. Miller (1996) has proposed a model to explain the observed bursting pulsar phase shifts. He assumes that the neutron star spin axis and the magnetic dipole moment are not aligned, breaking the azimuthal symmetry of the mass accretion and thus making the accretion column more of an accretion curtain, with a footprint on the stellar surface in the form of an arc. He assumes that some type of disk instability opens a gate that allows a sudden increase in the mass accretion rate. When the instability occurs, there is a temporary increase in the accretion torque that results in the dragging of the field lines at the inner edge of the disk and thus a deformation of the field lines. The field lines at the preferred azimuth for “pick up” of matter will then connect to a shifted footpoint on the neutron star surface. The corresponding change in the orientation of the accretion curtain will result in a change in the pulse phase.

We have shown that the average maximum phase shift observed during the bursts remained constant throughout the first outburst (cf. Fig. 4), during which the burst peak flux varied by a factor of  $\sim 3.3$ . This shows that the magnitude of the phase shifts, and thus of the field line deformation, is independent of the mass accretion rate during the bursts. Since both the persistent flux and the burst peak fluxes increase and decrease during the outburst, approximately in lockstep, it is possible that the deformation of the field lines is determined not by the mass accretion rate but by the relative mass accretion rate in units of its persistent (equilibrium) value. Alternatively, our results raise the possibility that the bending of the field lines is not caused by the sudden increase in the mass transfer rate but that the bending of the field lines and the increased mass inflow are both caused by one and the same instability. Once the instability occurs, the matter is allowed to travel along the deformed field lines, resulting in a phase shift in the pulsed emission during the burst. If this is the case, then the mechanism by which the phase recovers is unclear.

We thank Robert Mallozzi for many useful discussions, Mark Finger for providing the ephemeris for the persistent emission, and Kim Deal for her careful work in creating and making available a catalog of all GRO J1744–28 bursts observed with BATSE. T. K. and C. K. acknowledge support under NASA grant NAG 5-2560. J. v. P. acknowledges support under NASA grants NAG 5-2755 and NAG 5-3674. W. H. G. L. gratefully acknowledges support from NASA.

#### REFERENCES

- Briggs, M. S. 1996, in MIT GRO J1744–28 Workshop, Boston, MA  
 Finger, M. H. 1996, in MIT GRO J1744–28 Workshop, Boston, MA  
 Finger, M. H., Koh, D. T., Nelson, R. W., Prince, T. A., Vaughan, B. A., & Wilson, R. B. 1996, *Nature*, 381, 291  
 Fishman, G. J., et al. 1989, in Proc. *GRO Science Workshop*, ed. W. N. Johnson (Greenbelt: NASA/GSFC), 2–39  
 Fishman, G. J., Kouveliotou, C., van Paradijs, J., Harmon, B. A., Paciasas, W. S., Briggs, M. S., Kommers, J., & Lewin, W. H. G. 1995, *IAU Circ.* 6272  
 Jung, G. V., et al. 1996, *IAU Circ.* 6321  
 Kouveliotou, C., et al. 1996a, *IAU Circ.* 6286  
 Kouveliotou, C., van Paradijs, J., Fishman, G. J., Briggs, M. S., Kommers, J., Harmon, B. A., Meegan, C. A., & Lewin, W. H. G. 1996b, *Nature*, 379, 799  
 Lewin, W. H. G., Rutledge, R. E., Kommers, J. M., van Paradijs, J., & Kouveliotou, C. 1996, *ApJ*, 462, L39  
 Miller, G. S. 1996, *ApJ*, 468, L29  
 Paciasas, W. S., Harmon, B. A., Fishman, G. J., Zhang, S. N., & Robinson, C. R. 1996, *IAU Circ.* 6284  
 Stark, M. J., Baykal, A., Strohmayer, T., & Swank, J. H. 1996, *ApJ*, 470, L109  
 Strickman, M. S., et al. 1996, *ApJ*, 464, L131  
 Walraven, R. 1984, in Proc. *Digital Equipment User's Soc.*  
 Woods, P. M., et al. 1998, in preparation